Progress In Electromagnetics Research C, Vol. 11, 183–198, 2009

A NOVEL ACTIVE ANTENNA BEAMFORMING NETWORKS USING BUTLER MATRICES

S. K. A. Rahim

Wireless Communication Centre, Fakulti Kejuruteraan Elektrik
Universiti Teknologi Malaysia
81310 UTM, Skudai, Malaysia

P. Gardner

Department of Electronic, Electrical & Computer Engineering
The University of Birmingham
Edgbaston, B15 2TT, UK

Abstract—In this paper, a novel architecture of using cascaded Butler Matrices (BM) integrated with Low Noise Amplifiers (LNAs) is proposed. By using the narrow beams available from the Butler Matrix, it is possible for a receiver to increase the gain in the desired signal directions and reduce the gain in interference directions. Hence, high-gain narrowbeam signals for long-range application are produced. A novel technique is introduced which uses high linearity LNAs and a second Butler Matrix, acting as a mirror of the first Butler Matrix, reconstructing the antenna patterns of the individual radiating elements. The resulting outputs have high linearity and broad beam width that can be used for short-range communication. Design of the Butler Matrix, Low Noise Amplifier, Wilkinson Power Divider and High Linearity Low Noise Amplifier are presented in this paper. A final design of active antenna beamforming network using cascaded Butler Matrices integrated with LNAs is proposed. The beamforming network provides a method, which could be applicable in vehicle communication systems, where long-range communications with roadside beacons and short-range communications with the fast moving vehicle are both required.

Corresponding author: S. K. A. Rahim (sharulkamal@fke.utm.my).

1. INTRODUCTION

An Intelligent Transportation System (ITS) is a system based on wireless communication. ITS plays a significant role in improving the efficiency and safety of the transportation system. The system combines all aspects of technology and system engineering concepts in order to develop and improve transportation system of all kinds [1]. ITS, which utilize information and communications technology in vehicle as well as within the roadside infrastructure, can be used to improve mobility while increasing transport safety, reducing traffic congestion, maximizing comfort and reducing environmental impact [2]. There are various forms of wireless communications technologies proposed for ITS, which include short range and long range wireless communication systems. The short-range communications can be accomplished by using the Dedicated Short Range Communications (DSRC) standard [3, 4]. Alternatively, longer range communications for vehicle applications are proposed by using infrastructure networks such as Worldwide Interoperability for Microwave Access (WiMAX), Global System for Mobile Communications (GSM) or even the 3G system [5].

Butler Matrix has largely been used with various techniques such as waveguide [6], microstrip [7], multilayer microstrip [8] and CPW [9]. Butler Matrix is the key component of beamforming network, which is widely applied in smart antennas [10]. It increases the system capacity and provides higher signal to interference ratio, consequently enhancing the overall system performance [11]. Several studies have been conducted related to the Butler Matrix. Zak, Piovano and Angelluci introduced cascaded Butler Matrices in Multi-Port Amplifiers (MPAs) [12–14]. A signal entering one port of the Butler Matrix is divided into equal parts before the signal is amplified by all the amplifiers and then recombined by the combining Butler Matrix at the output port that corresponds to the particular input port. Suarez also used a Butler Matrix in his research [15, 16]. He reported a uniform narrowbeam switched array antenna system of up to eight beams, produced by means of cascaded passive Butler Matrices.

In this paper, cascaded Butler Matrices are integrated with Low Noise Amplifiers (LNAs) and High Linearity Low Noise Amplifiers (HL_LNAs). The objective of the proposed system is to produce high gain-narrow beam and high linearity-broad beam antenna systems that could provide multi-channel operation for diversity purposes in transport applications, particularly for roadside-vehicle and inter-vehicle communications. The details of the proposed system are

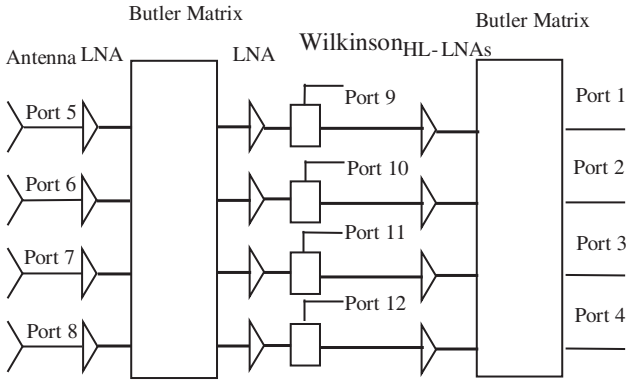

Figure 1. The block diagram of the active antenna beamforming network.

explained in Section 2.

2. EXPERIMENTAL CONFIGURATION

Figure 1 shows the block diagram of the front-end active antenna beamforming network system. The system was designed for applications at 2.45 GHz frequency range. The system consists of an array of patch antennas with 0.5λ spacing, LNAs, Wilkinson power divider, HL-LNAs and two Butler Matrices. The input ports of the architecture are referred to as Port 5 to Port 8. The output ports from the second BM are referred to as Port 1 to Port 4 while the output ports from the first BM are referred to as Port 9 to Port 12. The LNAs, HL-LNAs, Wilkinson power divider and Butler Matrices are fabricated on FR4 substrate with dielectric constant of 4.4.

Referring to the system configuration, signals received by the array antennas are amplified by identical first stage LNAs before entering the input ports of the first Butler Matrix. These signals are subdivided into equal amplitude with progressive phase variation across the output ports, for high gain-narrow beam reception. These signals are then re-amplified by the second stage identical LNAs before feeding into the Wilkinson power dividers. The signal from one end of each Wilkinson power divider forms a narrow output beam while the signals from the other ends of the Wilkinson power divider are fed to HL-LNAs to be amplified and recombined in the second Butler Matrix to regenerate the broad beam characteristics of the individual antenna elements. As a result, high gain and narrow beam signals are produced on the output ports of the first Butler Matrix while high linearity and

broad beam signals are produced on the output ports of the second Butler Matrix. When compared to a system involving direct, single ended amplification of the individual antenna outputs, this system offers enhanced linearity, because the outputs of the four high linearity amplifiers are power combined by the second Butler Matrix. The effect on the system noise figure of losses in the Butler Matrix is reduced with the introduction of LNAs before each stage of the first Butler Matrix [17]. The effects of interference, cross coupling and cross talk between the circuit elements in this experiment are reduced as the modules are shielded and partitioned with the metal boxes.

In addition to the multi-channel and multi-beam advantages produced by the proposed architecture, nulls at different angle could also be produced for the high linearity-broadbeam signals by alternatively switching off one of the HL-LNAs. This creates an adaptive array antenna system.

In conclusion, the proposed active cascaded Butler Matrices could form nine different beam patterns where four different beams are coming from the outputs ports of the first BM, one beam from any four of the output ports of the second BM while the other four different beams are formed from the output ports of the second BM which becomes a simple adaptive antenna system when individual HL-LNAs are turned off alternately. Figure 2 shows the image of the cascaded Butler Matrices system used in the measurements.

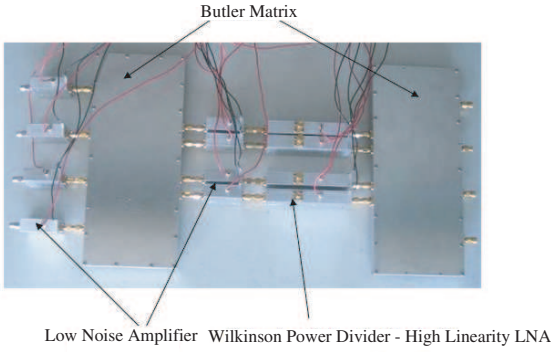

Figure 2. Image of the cascaded Butler Matrices system.

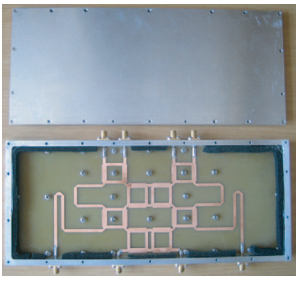

Figure 3. Image of the Butler matrix.

3. ELEMENTS OF THE ACTIVE ANTENNA BEAMFORMING NETWORK

3.1. Butler Matrix

Smart antennas provide a broad range of ways to improve the performance of wireless communication systems. Beamforming is one of the techniques that can be used in the system. RF beamforming techniques are divided into quasi-optic and circuit type [18]. The quasi-optic type uses a hybrid arrangement of either a reflector or lens objective with a feed array. The basic lens based beamforming are the Ruze lens and the Rotman lens [19, 20]. The circuit type beamforming technique uses couplers, phase shifter and transmission lines in order to create the multiple beam networks. Blass Matrix and Butler Matrix are two of the examples of the circuit based beamforming network [21, 22].

The Butler Matrix (BM) consists of N input ports with an equal number of output ports. A signal introduced at one input produces equal amplitude at all outputs but with a constant phase difference between them. As a result, the characteristic of BM can be used to control the direction of the beamforming of an antenna array at a certain angle in space. Figure 3 shows the image of the Butler Matrix as well as the shielded metal box used in this experiment. Absorbing carbon foams are attached to the sides and the underside of the top lid of the inner metal box in order to reduce internal coupling and external interference effects in the shielded metal box.

3.2. Low Noise Amplifier

The SNR at the output ports of the Butler Matrix can be increased with the introduction of LNAs. In the measurement, Agilent ATF-55143 amplifier with high dynamic range and low noise figure is used [23]. The chip is designed for use in low cost commercial application in the VHF through 6 GHz frequency range. They are duplicated and placed before and after the first stage BM in the cascaded Butler Matrices measurement.

Figure 4 illustrates the simulated and measured S-parameter results of the low noise amplifier. The simulated and measured results show good input return loss S_{11} around -10 dB at the resonant frequency of 2.45 GHz. The insertion loss S_{12} is better than -20 dB over the frequency range of 2 GHz to 3 GHz for both the simulated and measured results. The simulated gain from the output port S_{21} is 19 dB while the measured output signal is 17 dB. The slight discrepancy in the simulated and measured results can be associated with the tolerance of the dielectric permittivity of the FR4 substrates, etching problems

and inconsistency during the soldering processes. Figure 5 shows the image of the LNA shielded with the metal box to reduce coupling and interferences effects.

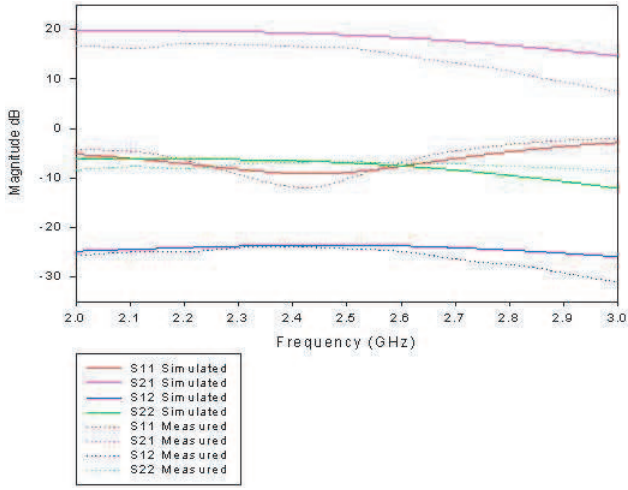

Figure 4. Simulated and measured S-parameter of the low noise amplifier.

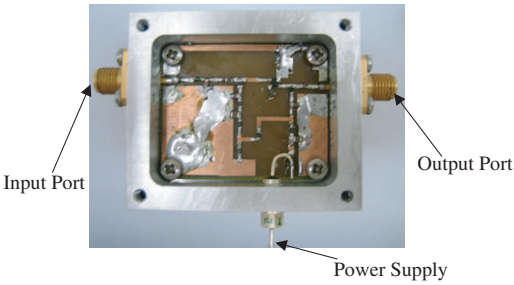

Figure 5. Image of the low noise amplifier.

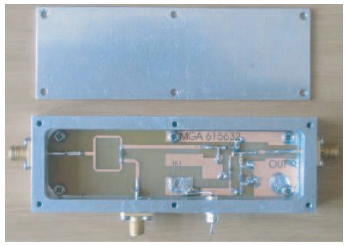

Figure 6. Image of the integrated Wilkinson divider and high linearity LNA.

3.3. Wilkinson Power Divider-high Linearity Low Noise Amplifier

The Wilkinson Power Divider-High Linearity Low Noise Amplifier modules (HL-LNAs) are used in the cascading Butler Matrices front-end system. One end of the Wilkinson Power Divider is used to produce high gain narrowbeam signal from the output port of the first BM while the other end of the Wilkinson Power Divider is used to supply the signal to the High Linearity Low Noise Amplifier to be fed to the second BM for recombining. Hence, high linearity broadbeam signals are produced from the outputs of the second BM.

Figure 6 shows the integrated Wilkinson Power Divider-High linearity low noise amplifier element. The element is duplicated and shielded with a metal box in order to reduce interference. The Wilkinson Power Divider is a lossy network commonly used for power splitting and combining. The power divider consists of $\lambda/4$ transmission line, which is equally split. One end of the divider is used to measure the output from the first BM while the second output port is connected to the HL-LNA. Avago Technology chip (formerly known as Agilent) model MGA-61563 is used as the HL-LNA [24]. The chip is an economical and easy to use GaAs MMIC amplifier that offers excellent linearity and noise figure for applications from 0.1 GHz to

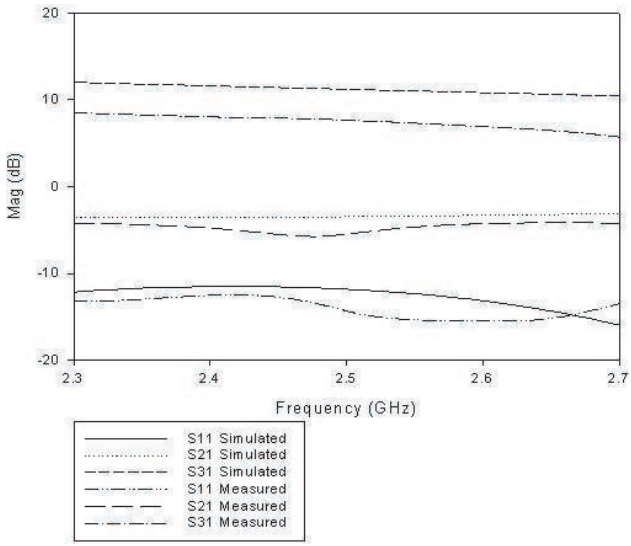

Figure 7. Simulated and measured S-parameters of Wilkinson power divider-high linearity LNA.

6 GHz. On-chip bias circuitry allows operation from a single +3 V or +5 V power supply.

Figure 7 shows the simulated and measured S-parameter results of the Wilkinson Power Divider-High Linearity Low Noise Amplifier. The simulated and measured results show good return loss S_{11} below −10 dB from 2 GHz to 3 GHz. The simulated and measured output signal from the output port of the Wilkinson Power Divider (S_{21}) is around −3 dB to −5 dB respectively. The simulated output signal from the amplifier, output Port 3 (S_{31}) at 2.45 GHz is 12 dB while the measured output signals from the same output port is 9 dB. The difference between the simulated and measured results is mainly due to etching process, soldering problems and losses due to FR4 substrates.

3.4. Microstrip Patch Antenna

In this experiment, the microstrip patch antenna is has been used as radiating element. The antenna is fabricated on FR4 board; the dielectric permittivity is 4.4 and thickness is 1.6 mm. Figure 8 shows the computed and measured input return loss S_{11} of the microstrip patch antenna. The simulation was performed using Agilent ADS software. The simulated and measured results show good return loss better than −20 dB at the resonant frequency of 2.45 GHz. The measured −10 dB bandwidth is about 70 MHz from 2.41 GHz to 2.48 GHz, which is about 2.9% from the centre frequency.

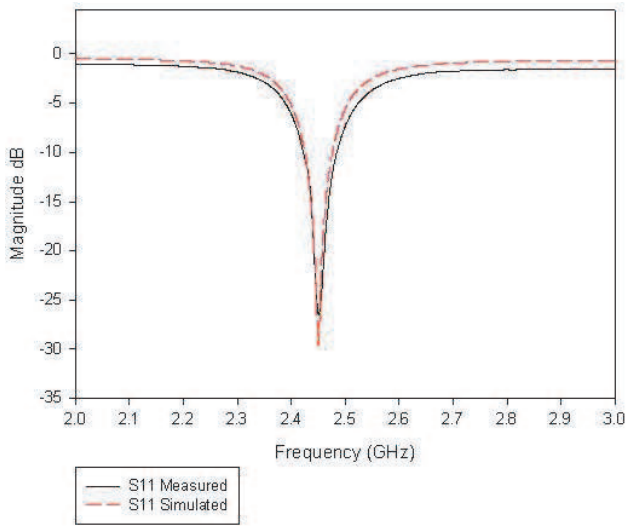

Figure 8. Measured input return loss of microstrip patch antenna.

4. RESULTS AND DISCUSSIONS

The radiation pattern measurement was carried out to show the narrowbeam and broadbeam antenna patterns of the system across 180° angles. The non-linearity measurement was also undertaken to investigate the advantage of the proposed cascaded Butler Matrices system as well as HL-LNAs.

4.1. Radiation Pattern Measurement

The radiation pattern measurements were conducted to illustrate the high gain narrowbeam and low gain broadbeam properties of the proposed receiver system. Referring to the block diagram of the proposed system, Figure 9 illustrates the simulated array factor from the output ports of the first Butler Matrix (Ports 9 to 12) and second Butler Matrices (Port 2) respectively. The input data for the simulated results were abstracted from measured S-parameter measurement. Table 1 shows the measured S-parameters from the first Butler Matrix and the cascaded Butler Matrices. Referring to the figures, beamforming patterns with peaks around $\pm 15°$ and $\pm 45°$ are generated from the output ports of the first Butler Matrix when input ports are fed with signals. Alternatively, broadbeam patterns are generated from the output ports of the second Butler Matrix when input ports are fed with signals.

The radiation pattern measurements from the output ports of the first Butler Matrix are shown in Figure 10. The results are compared

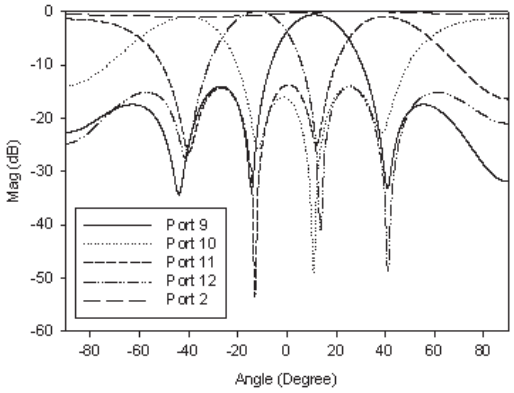

Figure 9. Simulated array factor from measured S-parameter of the broadbeam and narrowbeam.

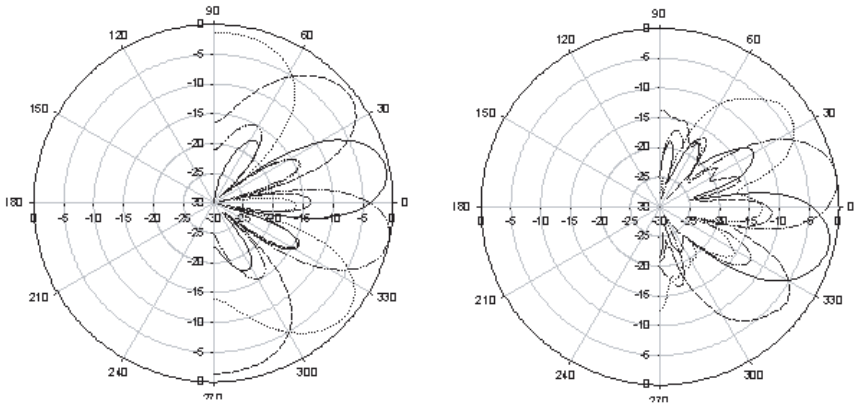

(a) (b)

Figure 10. (a) Simulated array factor and (b) measured beam pattern of narrowbeam.

Table 1. Measured S-parameter amplitude and phase at the output of first and second butler matrix.

Input Port / Output Port	Input Port 5	Input Port 6	Input Port 7	Input Port 8
	dB∟ Degree			
Output Port 1	17.7 ∟ 0°	12.2 ∟ –60.7°	19.1 ∟ –0.8°	33.6 ∟ –20.5°
Output Port 2	8.2 ∟ 0°	22.3 ∟ 178.8°	35.1∟ –107.3°	10.7 ∟ –81.1°
Output Port 3	18.1 ∟ 0°	34.7 ∟ –27.4°	22.7∟ 121.1°	18.0 ∟ –106.7°
Output Port 4	33.7 ∟ 0°	10.9 ∟ 171.3°	18.6 ∟ –80.1°	15.7 ∟ –167.7°
Output Port 9	18.3 ∟ 0°	18.7 ∟ 34.7°	19.4 ∟ –83.4°	18.5 ∟ –119.1°
Output Port 10	17.7 ∟ 0°	18.1 ∟ 138.3°	19.3 ∟ –89.9°	18.0 ∟ 52.3°
Output Port 11	19.1 ∟ 0°	19.1 ∟ –132.3°	18.1 ∟ 92.0°	18.0 ∟ –41.9°
Output Port 12	18.9 ∟ 0°	19.5 ∟ 47.2°	19.1 ∟ 94.4°	18.6 ∟ 130.4°

to the simulated array factor results. The measured radiation pattern results agree with the simulated array factor values in terms of the direction of the main beam. Generally, the measured main beams are more than 10 dB greater than the side lobes. Figure 11 shows the plots of measured radiation pattern from the output ports of the cascaded Butler Matrices as compared to the simulated array factor. It is clearly illustrated than when Butler Matrices are cascaded, broad beam signals will appear, as the individual antenna patterns are regenerated. The difference between the measured radiation pattern and the simulated array factor is mainly because the simulated array factor does not take into consideration the coupling effects.

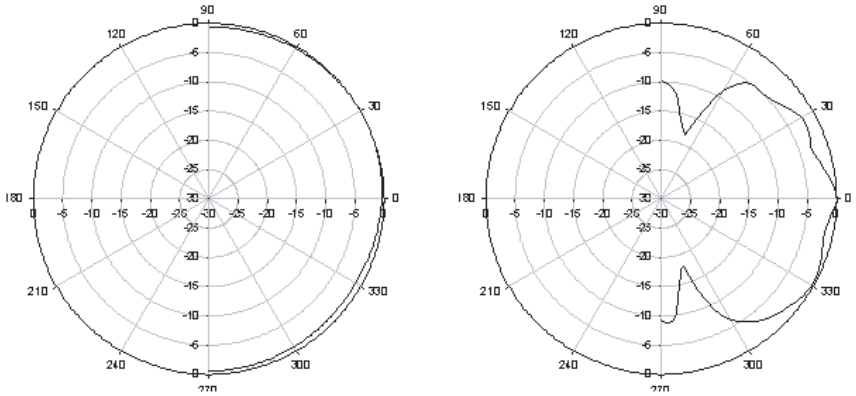

Figure 11. (a) Simulated array factor and (b) measured beam pattern of narrowbeam.

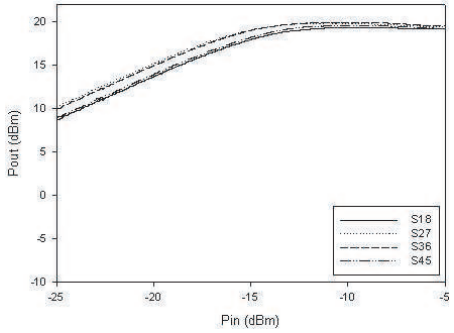

Figure 12. Non-linearity measurement outputs from the second Butler Matrix.

4.2. Non-linearity Measurement

In order to measure the linearity at the output ports of the proposed system, non-linearity measurement was conducted. Hewlett Packard network analyzer model 8722D was used to measure the gain of the output ports with swept input power. The measurement was conducted at a frequency of 2.45 GHz. In the measurement, output powers (P_{out}) are plotted against a range of input powers (P_{in}). The output powers are generated from (P_{out} = Gain $+P_{in}$).

Figure 12 shows the plot of output power from the output ports of the second BM (Output Port 1, Port 2, Port 3 and Port 4) against the

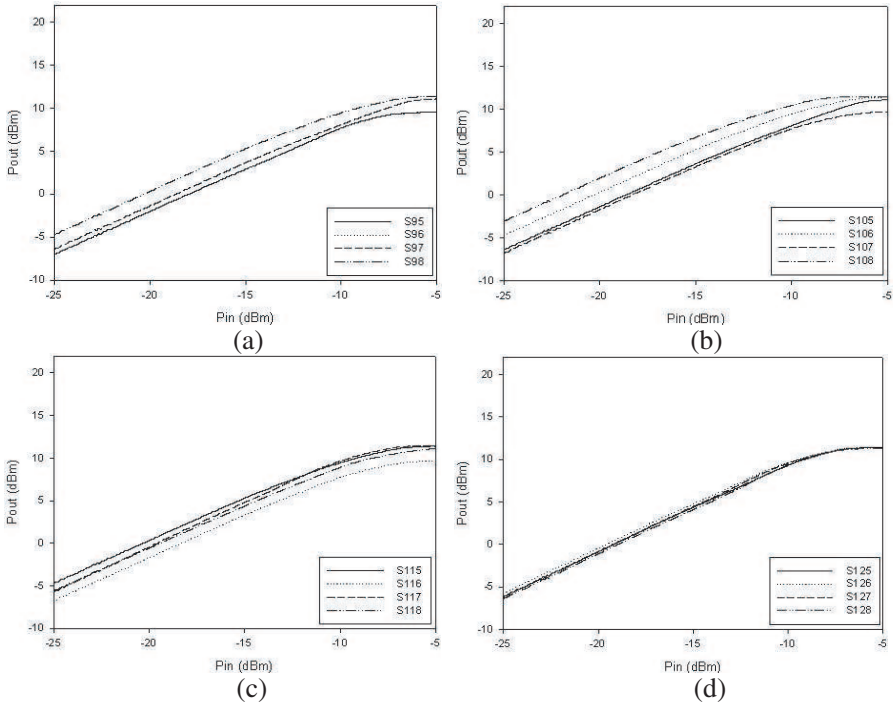

Figure 13. (a) Non-linearity measurement outputs from output Port 9. (b) Non-linearity measurement outputs from output Port 10. (c) Non-linearity measurement outputs from output Port 11. (d) Non-linearity measurement outputs from output Port 12.

input power (Input Port 5, Port 6, Port 7 and Port 8) when signals are fed to the input ports. These ports can be written as S_{18}, S_{27}, S_{36} and S_{45}. For example, S_{18}, as shown in legend on Figure 12, indicates that signal received by input port 8 is amplified, subdivided and recombined in order to regenerate the broad beam characteristics of the individual antenna elements in output port 1. On the other hand, Figure 13(a) to Figure 13(d) show the P_{out} against P_{in} from the output ports of the first BM (Output Port 9, Port 10, Port 11 and Port 12) when signals are fed to the input ports. In the measurement, a range of input power from -25 dBm to -5 dBm is fed to the input ports. The gain from each output port is abstracted in order to produce P_{out}.

In order to compare the linearity of the system between the output ports of the first and second BM, the 1 dB gain compression point is determined in the measurement. Figure 14 illustrates the non-linearity measurement when the input signals from the input ports of the first

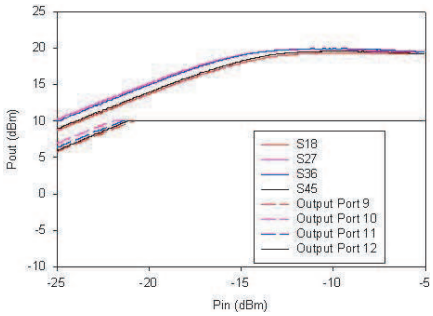

Figure 14. Non-linearity measurement outputs from the second butler.

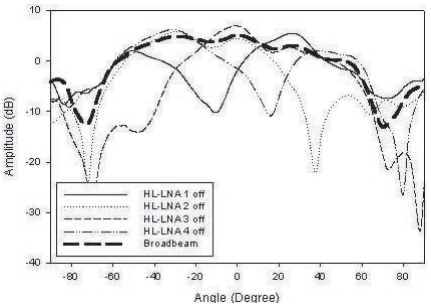

Figure 15. The adaptive measurement.

BM as shown in Figure 13 are recombined at the respective output ports. The results are compared to the output signals of the second BM. It is shown that for the output ports of the second BM, the measured input power at 1 dB gain compression is about -14 dBm, which corresponds to 19 dBm output power. On the other hand, the measured input power of the first BM is about -23 dBm, which corresponds to 10 dBm, output power. Hence, the 1 dB compression point of the first BM should be slightly lower than 10 dBm. The results clearly illustrate that the output from the second BM is much more linear compared to the output ports from the first BM.

4.3. Adaptive Antenna System Measurement

In this experiment, the HL-LNAs are switched off one by one. The objective is to illustrate the formation of nulls in the beams. Theoretically, the radiation pattern from the four output ports of the cascaded BM should produce the same radiation patterns; therefore only the radiation pattern output from Port 2 is used in this experiment.

Figure 15 illustrates the radiation pattern of the measured adaptive antenna system output from Port 2 when the HL-LNAs are switched off alternately. The results are compared to the pattern when all HL-LNAs are switched on. It is clearly shown that when one of the outermost HL-LNAs, namely either HL-LNA 1 or HL-LNA4 is switched off, a null is formed at angle around $\pm 15^\circ$ On the other hand, nulls are shown at angles around $\pm 35^\circ$ when HL-LNA 2 or HL-LNA 3 is switched off. It is concluded from this experiment that nulls could also be formed in the broadbeam angle with the proposed active cascaded BM system.

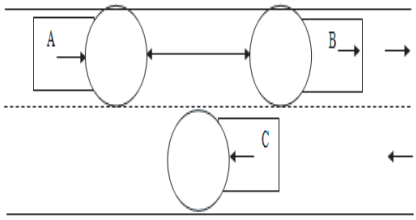

Figure 16. Three vehicles scenario.

The application of the adaptive antenna system can be illustrated as a three vehicles scenario as shown in Figure 16. Referring to the figure, two cars, Car A and Car B are moving in the same direction while car C is coming from the opposite direction. Car A and Car B are communicating between one another, and since the distance between the vehicles is small, a broadbeam channel is used because the cars are moving very fast. However, interferences are received from Car C that is coming from the opposite direction. With the adaptive antenna system, the configuration of communication system using the broadbeam channel between Car A and Car B does not need any change in order to suppress the interference from Car C instead one of the HL-LNAs can be switched off in order to maintain the communication between the vehicle and suppress the interference.

5. CONCLUSION

The novel architecture of using cascading BM integrated with LNAs is proposed. The study implements the concept that the first BM will act as a power divider that divides all the input power from the input ports. The second BM will act as a combiner that will re-combine the input signal from the first BM. LNAs are added before and after the first BM to increase the gain and to reduce the Noise power. The HL-LNAs are employed before the second BM to increase the linearity of the system. As a result, the output signals from the first BM, which acts as a beamforming network, have high gain and narrow beam width for long distance communication. While the outputs from the second BM, which acts as a mirror of the first BM, reconstructing the antenna patterns of the individual radiating elements, have high linearity and broad beam width, which can be used for short distance communication.

REFERENCES

1. Wang, F. Y., C. Herget, and D. Zeng, "Guest editorial developing and improving transportation systems: The structure and operation of IEEE intelligent transportation systems society," *IEEE Transactions on Intelligent Transportation Systems*, Vol. 6, No. 3, 261–264, Sep. 2005.
2. Andrisano, O., R. Verdone, and M. Nakagawa, "Intelligent transportation systems: The role of third generation mobile radio networks," *IEEE Communications Magazine*, Vol. 38, No. 9, 2000.
3. Jing, Z. and S. Roy, "MAC for dedicated short range communications in intelligent transport system," *IEEE Communications Magazine*, Vol. 41, No. 12, 60–67, 2003.
4. Inoue, H., S. Osawa, A. Yashiki, and H. Makino, "Dedicated short-range communications (DSRC) for AHS services," *Proc. IEEE Intelligent Vehicle Symposium*, 369–374, June 2004.
5. Barth, M., X. Lei, C. Yi, and M. Todd, "A hybrid communication architecture for intelligent shared vehicle systems," *IEEE Intelligent Vehicle Symposium*, Vol. 2, 557–563, 2002.
6. Alessandri, F., M. Dionigi, R. Sorrentino, and L. Tarricone, "Rigorous and efficient fabrication-oriented CAD and optimization of complex waveguide networks," *IEEE Trans. Microwave Theory and Tech.*, Vol. 45, 2366–2374, 1997.
7. Denidni, T. A. and T. E. Libar, "Wide band four port Butler matrix for switched multibeam antenna arrays," *Personal Indoor and Mobile Radio Communications, 14th IEEE Proceedings*, Vol. 3, 2461–2464, 2003.
8. Nedil, M., T. A. Denidni, A. Djaiz, and A. M. Habib, "A new ultra wideband beamforming for wireless communications in underground mines," *Progress In Electromagnetic Research M*, Vol. 4, 1–21, 2008.
9. Nedil, M., T. A. Denidni, and L. Talbi, "Novel Butler Matrix using CPW multilayer technology," *IEEE Trans. Microwave Theory and Tech.*, Vol. 54, 499–507, 2006.
10. He, J., B. Z. Wang, Q. Q. He, Y. X. Xing, and Z. L. Yin, "Wideband X band microstrip Butler Matrix," *Progress In Electromagnetic Research*, PIER 74, 131–140, 2007.
11. Liberti, J. C. and T. S. Rappaport, *Smart Antenna for Wireless Communications: IS-95 and Third Generation CDMA Applications*, Prentice Hall, Upper Saddle River, NJ, 1999.
12. Zak, T. and K. Sache, "An integrated Butler Matrix in multilayer technology for multi-port amplifier applications," *14th*

International Conference on Microwaves, Radar and Wireless Communications, Vol. 1, May 2002.

13. Piovano, P., L. Accatino, A. Angelucci, T. Jones, P. Capece, and M. Votta, "Design and breadboarding of wideband $N \times N$ Butler matrices for multiport amplifiers," *Microwave Conference/Brazil, SBMO International*, Vol. 1, 175–180, 1993.
14. Angelucci, A., P. Audagnotto, P. Corda, and B. Piovano, "Multiport power amplifiers for mobile-radio systems using microstrip Butler matrices," *Antennas and Propagation Society International Symposium, 1994. AP-S. Digest*, Vol. 1, 628–631, Jun. 1994.
15. Sudrez-Fajardo, C., M. Ferrando-Batallur, A. Valero, and V. Rodrigo, "Multiple beam system with circular arrays," *Antennas and Propagation Society International Symposium, 2005 IEEE*, Vol. 4B, 35–38, Jul. 3–8, 2005.
16. Suarez, C., M. Ferrando-Bataller, and A. Valero-Nogueira, "Pattern synthesis of uniform circular arrays with directive elements," *Antennas and Propagation Society International Symposium, 2004. IEEE*, Vol. 3, 2812–2815, Jun. 20–25, 2004.
17. Nibler, F., *High Frequency Circuit Engineering*, The Institute of Electrical Engineering, 1996.
18. Hall, P. S. and S. J. Vetterlein, "Review of radio frequency beamforming techniques for scanned and multiple beam antennas," *IEE Proceeding*, Vol. 137, No. 5, 293–303, 1990.
19. Ruze, J., "Wide-angle metal plate optics," *Proc. of the IRE*, Vol. 38, No. 1, 53–59, 1950.
20. Rotman, W. and R. Turner, "Wide-angle microwave lens for line source applications," *IEEE Trans. on Antennas and Applications*, Vol. 11, No. 6, 623–632, 1963.
21. Moody, H. J., "The systematic design of the Butler Matrix," *IEEE Transactions on Antennas and Propagation*, Vol. 12, No. 6, 786–788, 1964.
22. Blass, J., "Multidirectional antenna — A new approach to stacked beams," IRE Inter. Convention Record, Vol. 8, 1960.
23. Data Sheet Agilent ATF-55143 Low Noise Enhancement Mode Pseudomorphic HEMT in a Surface Mount Plastic Package.
24. Data Sheet, Avago Technologies MGA-61563 Current Adjusted, Low Noise Amplifier.